International Research Journal of Multidisciplinary Scope (IRJMS), 2025; 6(2): 1103-1111 IRJMS

Original Article | ISSN (O): 2582-631X DOI: 10.47857/irjms.2025.v06i02.03710

Evaluating the Potential of Cordycepin as a Therapeutic Agent for Cancer: In-Silico Analysis of EGFR and VEGFR Interactions

Sonit Kumari, Alok Kumar Malviya*

Applied and Industrial Biotechnology Laboratory, Department of Life Sciences, CHRIST (Deemed-to-Be University), Bangalore, Karnataka, India. *Corresponding Author's Email: Alokmalviya@gmail.com

Abstract

Due to multipotent activity, Cordycepin, a nucleoside isolated from Cordyceps fungi (*Cordyceps militaris*), has recently attracted considerable interest as a compound for antitumor. Cordycepin is also known as 3-deoxyadenosine, which is known to inhibit tumor growth, but the actual mechanism is not known. The present work aims to evaluate the cordycepin as an anticancer candidate by analyzing its impact on the major oncogene receptors EGFR and VEGFR through an in-silico approach. In the analysis, computational docking was performed with AutoDock Vina 1.5.7, which estimated the binding constants of cordycepin with EGFR and VEGFR and got binding energies of -6.8 kcal/mol and -5.5 kcal/mol, respectively, relative to a reference Leucovorin molecule. In addition, molecular dynamics simulations were also performed for the best complex (Cordycepin-EGFR) to examine the conformational dynamic behavior of the cordycepin-EGFR complex. The functionality and architecture of the cordycepin-EGFR complex were illustrated: their interaction might serve as a base for therapy. Also, ADMET predictions show that cordycepin follows Lipinski's rules, which supports the drug-likeness of cordycepin compounds. Accordingly, the findings presented here will confirm and draw the attention of the scientific community to use the cordycepin as a possible treatment for cancer and its potential use in scientific pharmacology.

Keywords: ADMET, Cordycepin, EGFR, Molecular Docking, Molecular Dynamic Simulation, VEGFR.

Introduction

Day by day, the growth of cancer cases is increasing steadily and impacting the death scenario of humans worldwide (1). Cancer is an abnormal growth of cells with the potential to metastasize (2). There are various systematic treatment methods that have been developed for the treatment of cancer by complete removal of a cancer cell (surgical removal), radiation therapies, or exerting a controlled death of cancer cells by using some antiproliferative drug via blocking the cell cycle (2). Systematic therapy might have side effects on normal cells as well; to avoid the side effects of drugs, scientists are trying to develop herbal remedies for the treatment of cancer such as cordycepin is one of the emerging herbal anticancer therapies (3). Cordyceps is a genus of parasitic fungus known for medications in China for over 300 years and is usually called 'Dong Chong Xia Cao' (4). Cordyceps species accommodate bioactive ingredients, in which cordycepin one of the major components is that exhibit potential therapeutic characteristics for cancer (5). Cordycepin is a nucleoside adenosine analogy, an active ingredient isolated from liquid cordyceps (Chinese medicinal mushroom) (6). Cordycepin is also known as 3-deoxyadenosine, this is a group of adenosines that plays a crucial role in intracellular and extracellular signaling pathways in various types of cells, tissues, and organs (7). Cordycepin is very much known to increase the cell apoptosis time-dependently by decreasing the cell cycle of the G2/M phase which indicates that cordycepin tends to inhibit cancer cells' mitosis and EGFR signaling (8). In addition, cordycepin is also known to inhibit the enhanced IL-17A in the cancer cell, which promotes DNA synthesis in cancer cells (8). EGFR is one of the important receptors that play a role in tumor proliferation, often overexpressed in various tumors such as lung, renal, colon, and pancreatic cancers. EGFR is activated by the epithelial growth factor, which triggers the RAS and mitogen-activated protein kinase cascade reaction and leads to tumor proliferation, division, and angiogenesis (9). A Leucovorin which is also referred to as folinic acid or citrovorum factor is a

This is an Open Access article distributed under the terms of the Creative Commons Attribution CC BY license (http://creativecommons.org/licenses/by/4.0/), which permits unrestricted reuse, distribution, and reproduction in any medium, provided the original work is properly cited.

(Received 05th January 2025; Accepted 17th April 2025; Published 30th April 2025)

remedy that is being employed constantly to minimize the side effects of methotrexate and other related chemotherapy treatments (Figure 1). Merely it is a kind of folic acid that belongs to B vitamin that is required by the body to form as well as replace new ones. Leucovorin helps to deliver folate to the body such that it helps the normal body tissues to withstand the effects of chemotherapy while, on the other hand, the cancer cells are affected more effectively. Leucovorin potentiates the 5-FU antitumor effect by overriding the thymidylate synthase in tumor cells though it has few general side effects such as stomatitis, anorexia, leucopenia, and skin rash (10).

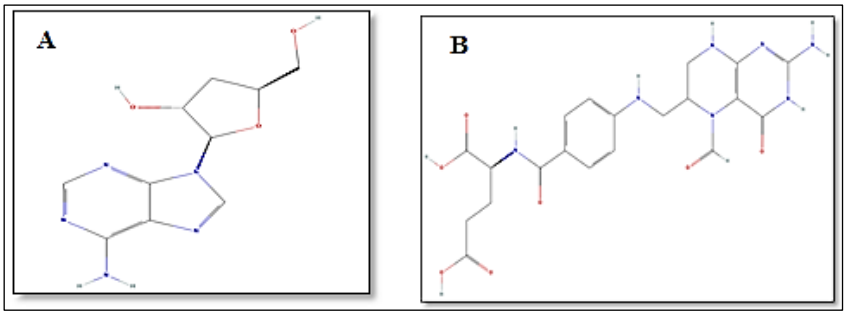

Figure 1: Molecular Structure of A) Cordycepin (C10H13N5O3) B) Leucovorin (C20H23N7O7)

The combination of leucovorin with methotrexate has been employed in the treatment regimens of many types of cancer including, colorectal cancer, breast cancer, and some kinds of leukemia. It is also applied for the treatment of toxicity of methotrexate and for the increased effectiveness of fluorouracil (5-FU) in particular types of cancer (11). However, leucovorin as an anticancer agent in combination therapy with 5-fluorouracil is sometimes employed in treating other diseases such as megaloblastic anemia, resulting for folate deficiency. This is easily available in the form of tablets, injections, and oral liquids. Such are the side effects of any medication, including leucovorin; but, typically, such as nausea, vomiting, diarrhea, and allergic reactions are not frequent. Currently, computational biology is one of the initial approaches towards understanding the mode of action of any novel molecule since computational docking is quite popular in the analysis of protein-ligand binding. Usually, Autodock Vina is applied in computational docking, which normally begins with preparing the target structure of the drug and receptors. Autodock is a set of programs that may be employed to recognize interaction disposition with the corresponding target.

Methodology

Preparation of Ligand

The molecular docking was performed by using Autodock Vina 1.5.7. To prepare the ligand for docking, spatial coordinates of constituent atoms in the 3D form of Cordycepin were retrieved from PubChem databases in the spatial data file (SDF) (https://pubchem.ncbi.nlm.nih.gov/). The SDF format of the ligand was opened in PyMOL 2.5 viewer and exported in the Protein data bank (PDB format). Further, the pdbqt file of the ligand was generated by using Autodock Vina 1.5.7 and saved in one folder.

Preparation of Protein

The 3D structure of proteins (receptors) has been obtained from RCSB PDB databases (https://www.rcsb.org/) and the PDB file of each protein was downloaded in the PDB format. PyMOL version 2.5 was used for a quick view of the 3D structure of each protein (12). This PDB format has been opened in AutoDock Vina 1.5.7 and preparation was done by removing water molecules, adding polar hydrogen followed by the addition of Kollman charges to the protein. Finally saved in the pdbqt file for the grid preparation.

Preparation of Grid

The pdbqt file of ligand and protein was opened in AutoDock Vina 1.5.7 and the grid box was inserted with less than 1Å spacing and x, y, and z coordinates to establish the size of the protein for docking, and the config file was generated in txt. Form and save in the same folder.

Molecular Docking

The molecular docking server was used to calculate the binding energies during protein and ligand interaction. The Auto grid program

generated a grid map of 40 X 40 X 40 Å grid points with a spacing of 0.375 Å (13). Command prompts were used to generate the docking results (14). Nine different runs were configured for each molecule and the lowest energy of affinity was considered for further evaluation.

ADME and Drug-Likeness Prediction

ADME stands for adsorption, distribution, metabolism, exertion, and toxicity which was predicted for cordycepin by using the pkCSM pharmacokinetics tool (http://biosig.unimelb.edu.au/ pkcsm/) were extracted and used as input of ADME prediction (15). The molecule was screened by ensuring no more than 5 H-bond donors (the total number of nitrogen-hydrogen and oxygen-hydrogen bonds) and 10 H-bond acceptors (all oxygen or nitrogen atoms), provided the molecular mass does not exceed 500 Da and octanol-water partition coefficient (log P) is less than 5. These parameters were used to determine the drug-likeness of Cordycepin (16). A boiled egg plot generated by the SWISSADME web tool which is one of the statistical visualizations. This shows the BBB (blood-brain barrier) and gastrointestinal permeability of drugs (17).

Molecular Dynamic Simulation

The molecular dynamics simulation (MDS) was carried out by using Gromac V.16 to investigate the stability of the protein-ligand complex, where cordycepin shows the best binding energies with EGFR (18). The selected ligand and receptor topology were downloaded from Amber and Poisson Boltzmann calculation was performed using an internal PBSA solver in the sander for force field calculation (19). The molecular dynamic simulation was performed with docking possess which were obtained from molecular docking of ligands and receptors and the best complex was selected. MDS was performed for ligand-protein complex and apo-protein and RMSD and RMSF graph was plotted.

Results and Discussion

Cordycepin Blocks the EGFR and VEGFR for the Treatment of Cancer

The possible cancer-inhibitive action can be assessed based on the capability of cordycepin in the regulation of receptors including EGFR and VEGFR in the malignant cells. Considering the first point the ligand molecule cordycepin has already been found to have anticancer activity. It has been described that cordycepin can inhibit the proliferation of cancer cells through the folding up of the EGFR. According to the literature, cordycepin will affect the escalation of cell apoptosis by down-regulating p-EGFR, p-Erk1/2, p-STAT3, p-p70 S6K, β-catenin, and cyclin B1 and up regulating p-STAT1 in 4NAOC-1 cells (19). As depicted under in-silica docking analysis in the current study, this research demonstrates the binding of the cordycepin to the EGFR and VEGFR (Table 1). In total, these outcomes give credence to our research hypothesis that cordycepin reduces further development of cancer cells under consideration of EGFR receptors (19). The binding energies of docked receptors are mentioned in **Error! Reference source not found.** which was calculated using Autodock Vina tool 1.5.7 which is represented in kcal/mol. Docking of Ligand and target protein can show the interaction affinity, which can result in inhibition of the proliferation of cancer cells. In the above error reference not found. Cordycepin and leucovorin have shown a total of 9 interactions with EGFR and VEGFR.

Table 1: Molecular Docking of Cordycepin and Leucovorin with VEGFR and EGFR

Receptor	Ligand	No. of Interactions	Affinity (kcal/mol)	No. of H-Bond	Amino acids
VEGFR	Cordycepin	9	-5.5	1	Glu705, Lys702, Glu720, Arg728, Asp710, Val708, Thr708
EGFR	Cordycepin	9	-6.8	1	Cys311, Glu317, Ala313, Ser315, Val336, Ser364, Thr402
VEGFR	Leucovorin	9	-5.5	1	-
EGFR	Leucovorin	9	-8.2	6	Glu319, Tyr316, Arg324, Glu317, Glu400, Cys311, Ala310, Ser366, Ser364, Val336, Thr364, Arg334

Visualization of all Docking

In Figure 2, Figure 3, Figure 4, and Figure 5, are showing interactions between the proteins which are illustrated using the tools of docking visualization as well as geometric illustrations of the target proteins. The docking visualization probably presents the anticipated ligand (like cordycepin or Leucovorin) to bind with the target proteins (EGFR and VEGFR) and the geometric representation demonstrates the structural form of the interacting peptide (target protein). The H-bond plots probably present all the hydrogen bonding between the amino acids of the target proteins and the ligand molecule. These plots are important for general reasons but particularly so as it provide more detail of the molecular interactions. 2D interaction plots focus on each of the amino acid-carbon involving the ligand molecule often depicted at the center. These plots give precise information on the residues of the protein that are involved in binding and their positioning relative to the ligand. Cordycepin and leucovorin structural description is done in ball and stick model and all the interactions of carbon amino acids are numbered and cited differently. This is useful in the identification of the various modes of bindings as well as the extent of interactions between the ligand and the target proteins. In general, these five visualizations help to clarify the ligand-target protein binding and may help to reveal the possible ways of the ligand's action and further research in the field of drug design.

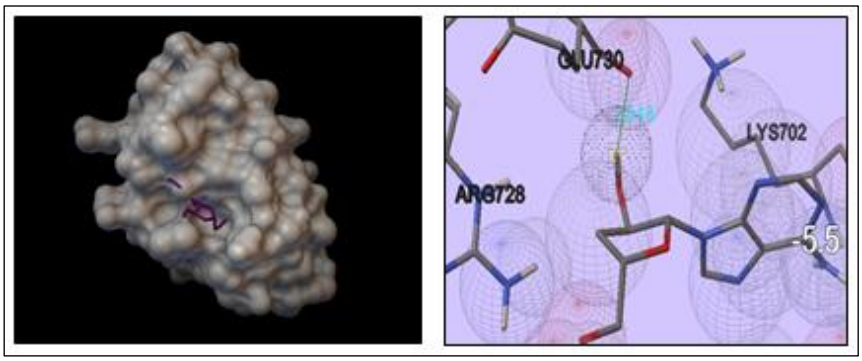

Figure 2: Visualization of Docking Visualization Leucovorin and VEGFR

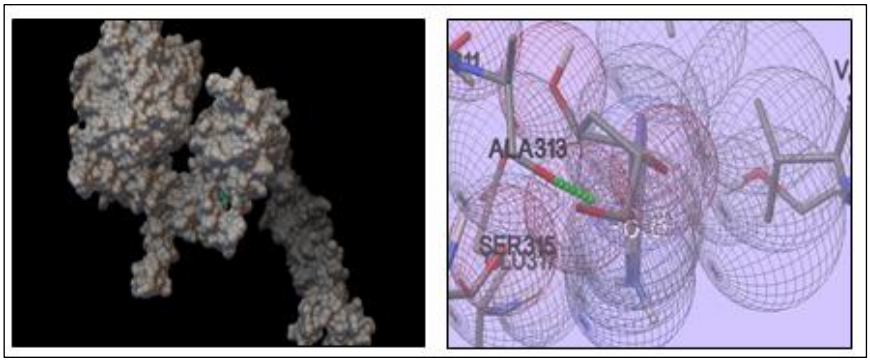

Figure 3: Visualization of Docking Visualization Leucovorin and EGFR

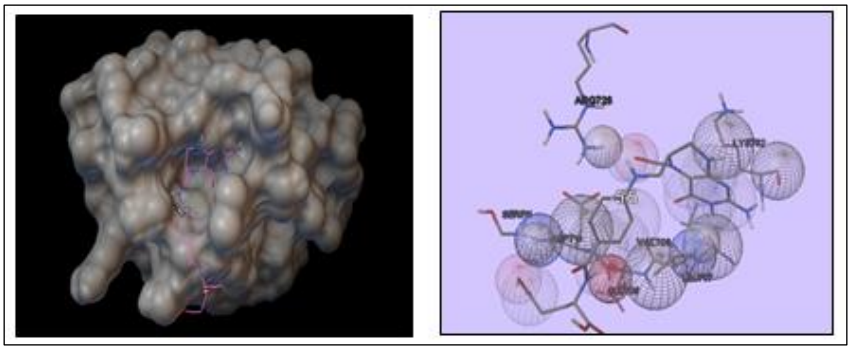

Figure 4: Visualization of Docking Visualization Cordycepin and VEGFR

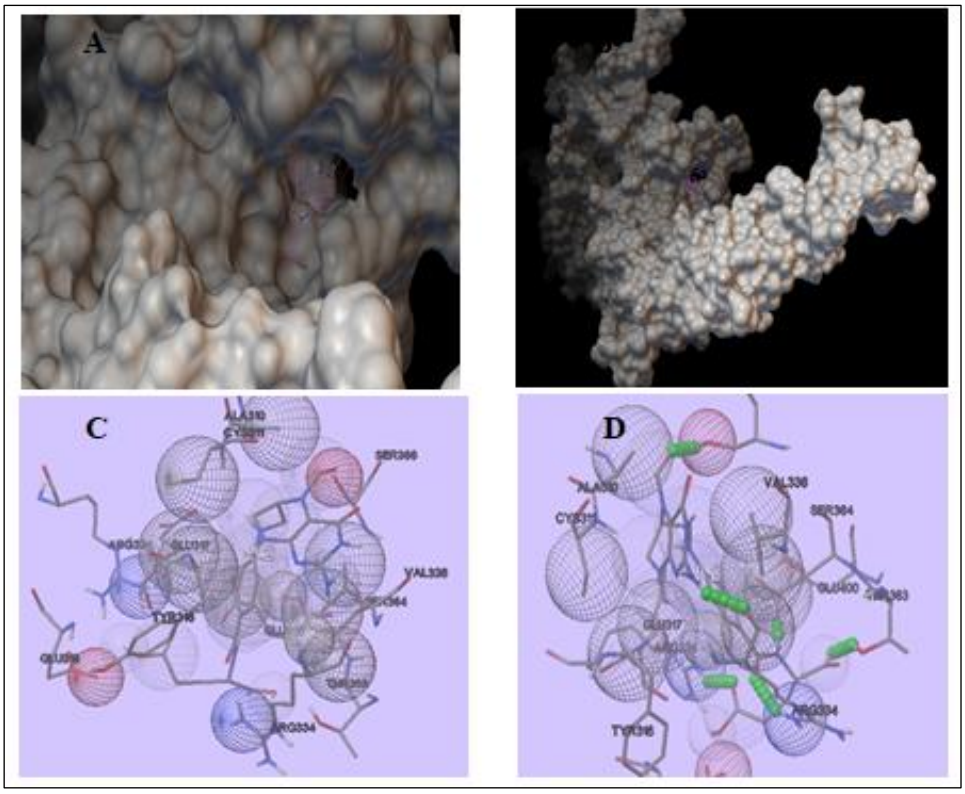

Figure 5: Visualization of Docking Visualization of Cordycepin and EGFR

ADME Prediction

The ADMET studies of the cordycepin indicated that the compound was compatible with the Lipinski's rule overload test in the first scan. The molecular weight of cordycepin was found by 237. 259 Da and a Log P value of -0. 1161, 6 H-bond acceptors, 4 H-bond donors of which 1 was a rotatable bond and a polar surface area of 98. 596 Å2. Further, the molecular weight was calculated to be less than 500 Da along with less than 10 H-bond acceptors, 5 H Bond donors, and the value logP was less than 10, which also gave an inference of the cordycepin as a compatible druglike. The output of data displayed in the table was in Table 2 below.

Table 2: Boiled Egg Plot by SWISSADME

PubChem ID	ME (g/mol)	TPSA (A^2)	MLOP	GI absorption	BBB permeant
Leucovorin	473.44	219.84	-0.62	Low	No
Cordycepin	251.24	119.31	-1.94	High	No

In the case of the boiled egg plot, SWISSADME was employed in establishing the proficiency and efficiency of small compounds in crossing the blood-brain barrier and the gastrointestinal barrier. Physicochemical spaces are categorized into three parts: Yellow (most likely to penetrate the BBB), white (designation of a compound that can permeate the gastrointestinal barriers), and grey (implies low absorption of a compound across both gastrointestinal and BBB). The comparison of cordycepin and leucovorin is stated on Table 2 and the graph is illustrated in Figure 6. More to the point, the compound cordycepin is in the white area which represents this compound that can cross the gastrointestinal barrier while leucovorin is located in the grey area which demonstrates poor absorption through both the blood-brain barrier and the gastrointestinal tract.

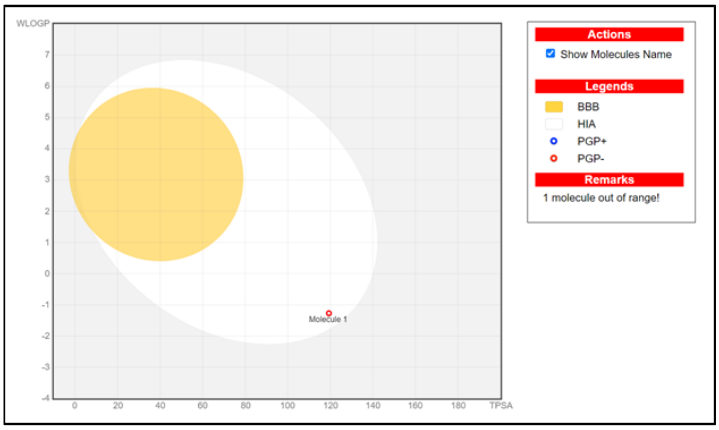

Figure 6: Boiled Egg Plot by SWISSADME

Molecular Dynamic Simulation

Cordycepin had a binding energy of negative six. This was about 90 kJ/mol when in association with EGFR, while leucovorin had a binding energy of -8.2 kJ/mol. Hence, based on their values of binding energy, leucovorin bound more actively and to a greater extent to EGFR than cordycepin. This would imply that leucovorin might perhaps be more sensitive to binding to EGFR and consequently, may contain the capacity to block the protein in case of cancer treatment (20). However, it should be borne in mind that energies obtained from docking are computed or predicted values, and may not always synchronize with the biological activities of the given compounds. However, this study would require some follow-up experimentation to establish the effectiveness of cordycepin and leucovorin in dealing with EGFR concerning cancer treatment.

The MD simulation was performed for use in the evaluation of the stability and conformational behavior of the atoms of the protein-ligand complex (21). Molecular dynamics simulation of the protein-ligand complex was performed for 100ns to measure thermodynamic stability in terms of Area; Root means square fluctuation (RMSF), Radius of gyration (Rg), and Root mean square deviation (RMSD). Please see Table 3 for individual energies of EGFR to cordycepin. Where ΔVDWAALS is -11. As mentioned above 55 Kj/mol is a change in van der Waals energy upon binding between a ligand and its target protein, while ΔEEL is 48. Reorganizations of 67 kJ/mol of electrostatic energy on ligand binding to its target protein. The fact that the root-mean-square deviation in energy will be positive for ΔEEL value will suggest that non-electrostatic interactions may tend to weaken the ligand-protein complex, thus, the binding interaction. In the molecular docking experiments, ΔGGAS is 37. 12 kcal/mol of Gibbs free energy of solvation during the binding between a ligand and the target protein. Therefore, a positive value of ΔGGAS implies that for binding to occur, solvation energy is not favourable, a sign that there might be problems in forming a stable complex. Refer to Figure 8 for a graphical representation of Molecular Dynamic Area, RMSD, RMSF, and Rg of APO protein and Protein-Ligand which is indicating APO protein is very much similar to protein-ligand.

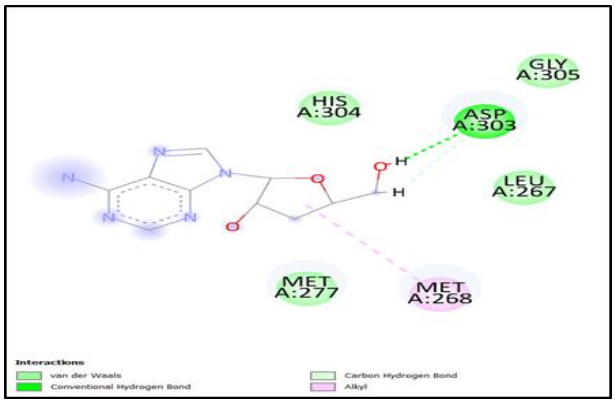

Figure 7: Interaction by Molecular Dynamic Simulation

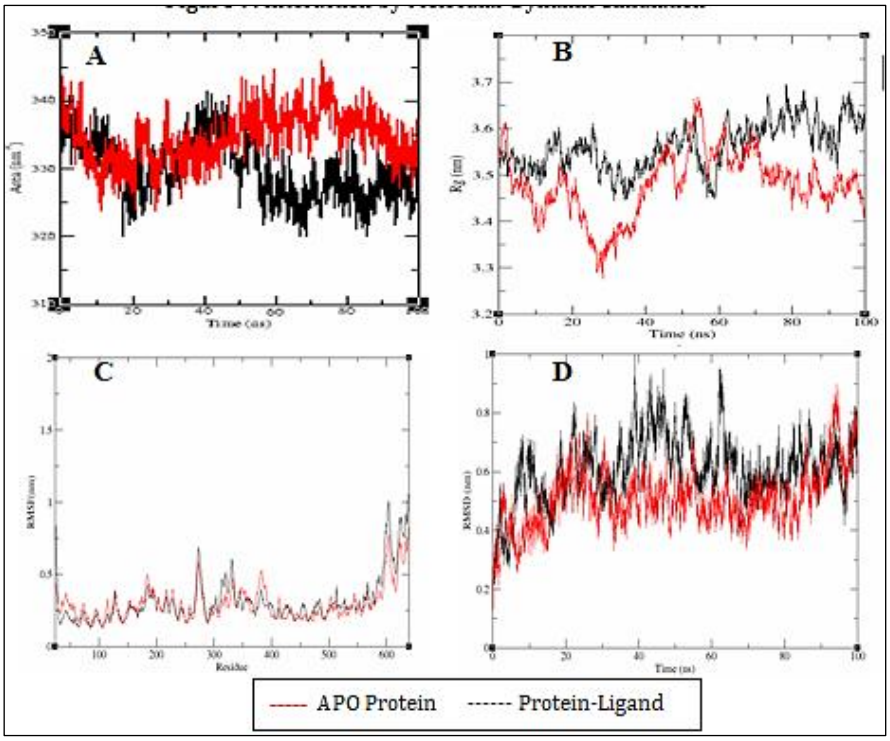

Figure 8: Molecular Dynamic Area, RMSD, RMSF and Rg

A negative ΔGSOLV value indicates a decrease in solvation energy on binding which means that the ligand-protein complex is better off than the solvated individual molecules. This means that the energy for the desolvation of the binding sites on the protein and the ligand and any water molecules that are displaced during the binding process will in the main contribute in a positive way to the overall stability of the complex encountered in this case.

Table 3: Energy Component of Protein-Ligand Complex

Energy Component	Protein-ligand complex		
	Average (KJ/mol)	SD	SEM
ΔVDWAALS(Van Der Waals Energy)	-11.55	0.71	0.36
ΔEEL(Electrostatic Energy)	48.67	8.26	4.13
ΔGGAS(Gibbs Free Energy of Solvation)	37.12	8.00	4.00
ΔGSOLV(Change in Solvation-Free Energy)	-44.03	7.31	3.65
ΔTOTAL	-6.90	0.96	0.48

The H-bond analysis that was performed with the help of trajectory acquired at 100 ns confirmed the presence of two hydrogen bonds between the ligand and the amino acid residue of the protein, namely Asp303 (Figure 7). Such a bond is a hydrogen bond, and it is said to occur when a hydrogen atom covalently bonded to an electronegative atom forms a bond with another electronegative atom. From the perspective of molecular docking, if the hydrogen bonds are formed between the ligand and specific amino acid residues of the protein binding site then it gives evidence of some crucial interactions responsible for the stability of ligand-protein complex. Alkyl interactions were observed with MET: 268 Also known as hydrophobic interactions where non-polar groups of the molecule or alkyl chains interact with each other or with non-polar parts of other molecules. These interactions are mainly of the van der Waals type with the dispersion force being the most dominant in this kind of cluster. A molecular dynamic simulation RMSD graph was used to analyze the deviation from the reference structure of the simulation where the RMSD was found to be average. From the result obtained, it was seen that 6nm was maintained throughout the simulation which makes it evident that the complex did not change throughout the simulation. A few fluctuations are noted when

analyzing the region between 40 ns and 70 ns of the simulation where RMSD moves up to 0. so there is an inconsistency: small 'distances' of 9 nm to 1 nm, imply a period of restructuring or reorganization of the complex. However, this structure oscillates up to 70 ns, and later, it is found to be in a stable state, confirming that a structural equilibrium has been maintained in this complex. For this reason, the RMSF graph offers information on the variation of specific amino acid residues in the protein-ligand complex. The average change was about 0.25nm from the simulation it was seen that the distance varied to as low as 0.25nm and the highest amplitude of oscillation of 1nm was recorded in amino acid residues ranging from position 600 to 638 implying that this part is more flexible than the rest of the complex. This evidence pertains to the RMSF pattern of the APO protein, the protein with no ligand and the protein-ligand complex exhibiting similarities in their dynamics of flexibility thus pointing to the fact that the presence of the ligand does not considerably alter the flexibility or dynamics of the protein. From the variation analyses of RMSD and RMSF, it can be inferred that the protein-ligand complex is rather stable during the whole duration of the simulation with slightly more vacillations in one or two areas.

Rg defines the extent of the coil – the lower Rg the more compact the molecular structure, and the more folded. Derived from the Rg graph, it is observed that the Rg values of the protein-ligand complex are normalized with values ranging from 3. 5 nm and 3nm. The radius of gyration (Rg) of the wild-type APO protein was determined to be 7 nm, and the Rg of the APO protein varies between 3. 3 nm and 3. 65 nm. The fact that Rg values calculated for the protein-ligand complex are smaller than the calculated for the APO protein reduces the propensity of conformational changes of the protein in the presence of the ligand, which suggests that the protein gets more compact in the presence of the ligand. SASA is defined as the extent of the molecule's surface concerning which solvent molecules can interact. In the SASA section on the SASA graph, the SASA values of the protein-ligand complex fluctuate between 320 nm^2 and 340 nm^2. The change in SASA in the health status of APO protein and the protein-ligand complex at first, are very close to each other, indicating complimenting properties of surface exposure. Of course, some of these differences can be observed only at a certain point in time, which suggests that the ligand may alter the accessibility of the protein surface.

Conclusion

The preliminary results of the molecular docking study indicate that cordycepin with EGFR and VEGFR has promising potential based on the docking results are presented here with comparison to leucovorin. But both molecules contribute less binding energy for EGFR (-6. 9 KJ/mol and -8. 2 KJ/mol) which is involved in cell growth and division and has its over-expression linked to various types of cancers. VEGFR has a great involvement in a process known as angiogenesis, or the formation of new blood vectors, which are highly influential in the growth and spread of cancerous cells in the body. The fact that cordycepin can bind to these receptors makes it possible for it to be therapeutic in the treatment of cancers. However, to confirm the effectiveness or IL-4 as a possible anticancer agent or not, further elaborate studies in cultures and animals would prove useful. Furthermore, the detailed study of the binding properties of cordycepin to the receptors may help in understanding the mode of action of the compound and the development of related drugs.

Abbreviations

ADME: Absorption, distribution, metabolism, and excretion, EGFR: Endothelial growth factor receptor, VEGFR: Vascular endothelial growth factor receptor.

Acknowledgment

We would like to thank Christ (Deemed to be University) for supporting and encouraging this research.

Author Contributions

Sonit Kumari: Making concepts, writing an article, making figure design, analyzing the data, finding references, Alok Kumar Malaviya: Evaluating article, reviewing article.

Conflict of Interest

The authors have expressed no conflict of interest.

Ethics Approval

Not applicable.

Funding

None.

References

1. Anderson BO, Flanigan J. Novel methods for measuring global cancer burden: Implications for global cancer control: Implications for global cancer control. JAMA Oncol. 2015; 1(4):425–7.
2. Yoon SY, Park SJ, Park YJ. The anticancer properties of cordycepin and their underlying mechanisms. Int J Mol Sci. 2018; 19(10):3027.
3. Liao Y, Ling J, Zhang G, Liu F, Tao S, Han Z, et al. Cordycepin induces cell cycle arrest and apoptosis by inducing DNA damage and up-regulation of p53 in leukemia cells. Cell Cycle. 2015; 14(5):761–71.
4. Yue K, Ye M, Zhou Z, Sun W, Lin X. The genus Cordyceps: a chemical and pharmacological review: A review of Cordyceps. J Pharm Pharmacol. 2013; 65(4):474–93.
5. Tian X, Li Y, Shen Y, Li Q, Wang Q, Feng L. Apoptosis and inhibition of proliferation of cancer cells induced by cordycepin (Review). Oncology Letters. 2015; 595–9.
6. Tan L, Song X, Ren Y, Wang M, Guo C, Guo D, et al. Anti-inflammatory effects of cordycepin: A review. Phytother Res. 2020; 35(3):1284–97.
7. Sheth S, Brito R, Mukherjea D, Rybak LP, Ramkumar V. Adenosine receptors: expression, function and regulation. Int J Mol Sci. 2014; 15(2):2024–52
8. Hsu PY, Lin YH, Yeh EL, Lo HC, Hsu TH, Su CC. Oncotarget 1 www.impactjournals.com/oncotarget Cordycepin and a preparation from Cordyceps militaris inhibit malignant transformation and proliferation by decreasing EGFR and IL-17RA signaling in a murine oral cancer model. 2017. www.impactjournals.com/oncotarget/
9. Patel D, Lahiji A, Patel S, Franklin M, Jimenez X, Hicklin DJ, Kang X. Monoclonal antibody cetuximab binds to and down-regulates constitutively activated epidermal growth factor receptor vIII on the cell surface. Anticancer Res. 2007; 27(5A):3355–66.
10. Wang S, Wang L, Zhou Z, Deng Q, Li L, Zhang M, et al. Leucovorin enhances the anti-cancer effect of bortezomib in colorectal cancer cells. Sci Rep. 2017;7(1)682.
11. Lunin VY, Urzhumtsev A, Bockmayr A, Fokin A, Urzhumtsev A, Afonine P, et al. Theory and Techniques 12. Binary Integer Programming and its Use for Envelope Determination Bulk Solvent Correction for Yet Unsolved Structures Search of the Optimal Strategy for Refinement of Atomic Models Metal Coordination Groups in Proteins: Some Comments on Geometry, Constitution and B-values: http://www.iucr.org
12. Lunin VY, Urzhumtsev AG. Improvement of protein phases by coarse model modification. Acta Crystallogr A. 1984; 40(3):269–77.
13. Morris GM, Ruth H, Lindstrom W, Sanner MF, Belew RK, Goodsell DS. Software news and updates AutoDock4 and AutoDockTools4: Automated docking with selective receptor flexibility. J Comput Chem. 2009; 30(16):2785–91.
14. Trott O, Olson AJ. AutoDock Vina: improving the speed and accuracy of docking with a new scoring function, efficient optimization, and multithreading. J Comput Chem. 2010; 31(2):455–61.
15. Daina A, Michielin O, Zoete V. SwissADME: a free web tool to evaluate pharmacokinetics, drug-likeness and medicinal chemistry friendliness of small molecules. Sci Rep. 2017; 7(1):42717.
16. Surya Ulhas R, Malaviya A. In-silico validation of novel therapeutic activities of withaferin A using molecular docking and dynamics studies. J Biomol Struct Dyn. 2022; 40(10):4691-4700.
17. Nayarisseri A, Abdalla M, Joshi I, Yadav M, Bhrdwaj A, Chopra I, et al. Potential inhibitors of VEGFR1, VEGFR2, and VEGFR3 developed through Deep Learning for the treatment of Cervical Cancer. Sci Rep. 2024; 14(1):13251
18. Abraham MJ, Murtola T, Schulz R, Páll S, Smith JC, Hess B, et al. GROMACS: High performance molecular simulations through multi-level parallelism from laptops to supercomputers. SoftwareX. 2015; 1–2:19–25.
19. Makarewicz T, Kaźmierkiewicz R. Molecular dynamics simulation by GROMACS using GUI plugin for PyMOL. J Chem Inf Model. 2013; 53(5):1229–34.
20. Rácz A, Mihalovits LM, Bajusz D, Héberger K, Miranda-Quintana RA. Molecular dynamics simulations and diversity selection by extended continuous similarity indices. J Chem Inf Model. 2022; 62(14):3415-25.
21. Hollingsworth SA, Dror RO. Molecular dynamics simulation for all. Neuron. 2018; 99(6):1129-43.